Journal of Bio- and Tribo-Corrosion (2022) 8:37
https://doi.org/10.1007/s40735-022-00638-4

Frontiers in Organic Corrosion Inhibitors for Chloride and Acidic Media: A Review

Wan Mohamad Ikhmal Wan Mohamad Kamaruzzaman[1,2] · **Nursabrina Amirah Mohd Nasir**[1,2] · **Nur Aiman Syafiq Mohd Hamidi**[1,2] · **Nusaibah Yusof**[1,2] · **Muhamad Syaizwadi Shaifudin**[1,2] · **Abdul Muiz Aniq Aiman Mohd Suhaimi**[1,2] · **Malia Athirah Badruddin**[1,2] · **Wan Mohd Norsani Wan Nik**[2,3] · **Mohammad Fakhratul Ridwan Zulkifli**[2,3] · **Azila Adnan**[1] · **Wan Rafizah Wan Abdullah**[2,3] · **Mohd Hafiz Mohd Zaid**[4] · **Khamirul Amin Matori**[4] · **Chen Soo Kien**[4] · **Pierluigi Traverso**[5] · **Roberto Stifanese**[5] · **Jiyaul Haque**[6] · **Mohd Sabri Mohd Ghazali**[1,2]

Received: 5 October 2021 / Revised: 7 January 2022 / Accepted: 19 January 2022 / Published online: 6 February 2022

Abstract

Metallic materials have propelled human advancements for centuries. Nevertheless, the rapid degradation of metallic structures in corrosive environments is inevitable. To date, the demand for metal alloys in multiple sectors, including construction and transportation, continues to escalate, with the trend it is predicted to reach beyond 250% by 2050. Thus, the need for corrosion inhibitors (CI) with qualities of high efficiency, excellent solubility, low toxicity, and inexpensiveness drive researchers to examine various possibilities. Here, we review the novelty, methods, and outputs from the latest studies on organic CI with the primary purpose of protecting mild steel and stainless steel in salt and acidic solutions. We reviewed the effectiveness, synergism impacts, and technological availability of each inhibitor and also comprehensively discussed related mechanisms of metallic corrosion and inhibition of CI.

Keywords Corrosion · Corrosion inhibitor · Steel · Acidic · Metalworking fluid

1 Introduction

Corrosion is a natural phenomenon that critically affects most of the industrial sectors such as refining and transportation industries [1, 2], nuclear facilities [3], food processing factories [4], marine infrastructures [5, 6], oil and gas buildings [7], industrial wastewater treatment system [8], metallic implants fields [9], and others. The process involves an electrochemical reaction between the metal surface and its surrounding corrosive environments like oxygen and water. Moreover, with the presence of corrosive agents, the oxidation of metal can be accelerated, and more electrons will be gained from the anodic site [10]. Numerous disadvantages of corrosion are linked to economic loss, structural failure, and catastrophic incidents. In 2019, a staggering amount of 614 pipelines incidents were reported in the United States, with the total death count of 10 people and injuries of more than 30. Figure 1 shows the cause and percent distribution of hazardous liquid line incidents from 2010 to 2019, as reported by the U.S. Department of Transportation.

An accurate estimation of global economic loss because of corrosion is difficult, but based on the information gathered by the National Association of Corrosion Engineers (NACE) International IMPACT, more than USD 2.5 trillion is lost in 2013, with up to 40% is due to the microbiologically influenced corrosion (MIC) [12]. Nonetheless, the severe effects of corrosion can be reduced if appropriate control methods are implemented from the early stages. An evaluation by NACE in 2016 suggested that a proper application of the corrosion control method should be able to reduce the economic loss from 15 to 35%, approximately between USD 375 billion to USD 875 billion [13]. Among the available practices such as cathodic protection, coatings, design, inhibitors, and material selection, inhibitors are the most popular for closed-system application in a chloride-concentrated solution. Furthermore, compared to other methods, the inhibitor does not need a high initial cost, does not need complex preparation methods, is easier to remove, and is

✉ Mohd Sabri Mohd Ghazali
mohdsabri@umt.edu.my

Extended author information available on the last page of the article

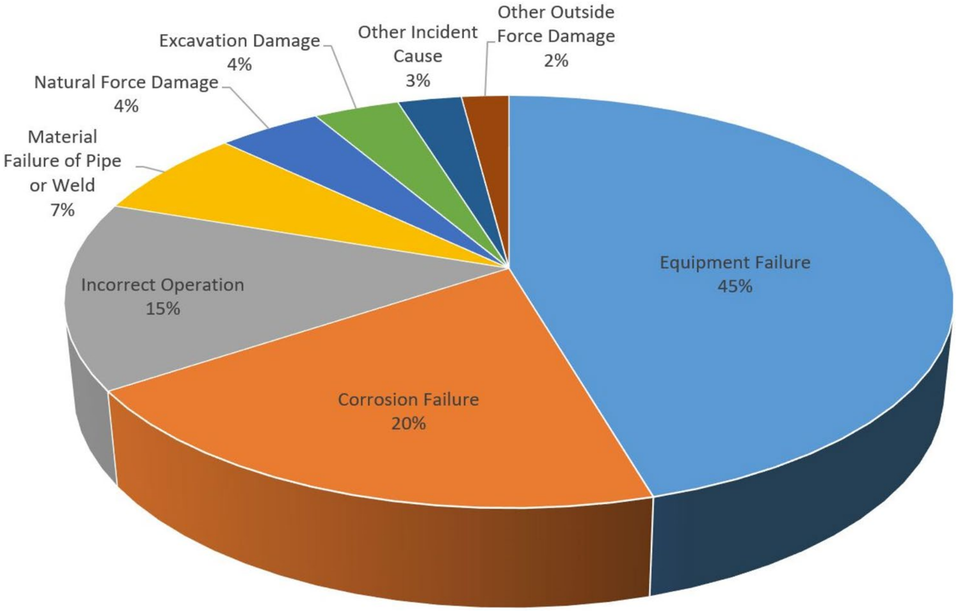

Fig. 1 Cause and percentage distribution of hazardous liquid line incidents 2010–2019 [11]

independent of external equipment. Corrosion inhibitor minimizes the degradation rate through an adsorption reaction on the metal surface, forming a thin monomolecular film that blocks direct contact with the surrounding aggressive elements [14]. Back in the day, synthetic organic CI and traditional inorganic CI were used without any concern on how it may affect human and aquatic life. The famous examples of hazardous inhibitors are tributyltin [15], cobalt octoate [16], chromates [17], and lead [18]. However, since the restriction imposed on these materials is legislated, it has prompted researchers to evaluate the available natural resources as a replacement with friendlier properties. This review paper assesses the trilateral view of corrosion, including sources of corrosion, corrosion mechanisms on mild and stainless steel, and recent development of organic CI to reduce the corrosion effects in chloride and acidic media.

2 Environmental Influences of Metallic Alloys

Metallic materials have persistently impacted human history and shaped our civilization. They have ushered in technological advancements with load-bearing applications for us to explore the harshest environment. No known materials have ever provided such a diversity of attributes in strength, resistance, conductivity, ductility, joinability, magnetism, and hardness. The versatility displayed by metallic materials enables various infrastructure, transportation, communication, and health applications. Recently, the development of metal alloys boosted the efficacy of several critical sectors such as transportation with the introduction of alloys having better strength and toughness, but low in weight [19, 20], a power station with a turbine that can operate efficiently under high temperature [21], a nuclear industry with more suitable components for safer waste disposal [22], biomedical implants for human with higher corrosion resistance [23], and embrittlement-resistant alloys for spacecraft usage [24]. The importance of metallic industries also signifies its significant impact on the environmental crisis. The success of these materials has pushed forward for large-scale industrial production, causing its availability to drop significantly over the years. Based on records and trends, the increasing urbanization, electrification, and digitization will consume more metallic materials when more than 60% of the population lives in cities by 2025. Furthermore, the production and usage of metal worldwide per year released up to 4.4 gigatons of carbon dioxide, CO_2 as a byproduct, equivalent to 30% of all the industrial sectors combined [25]. These factors proved that proper management to reduce the metal usage and amount of byproducts with risky potential to endanger the environment are crucial.

3 Mild Steel (MS)

MS (low carbon steel) is one of the most preferred metallic materials for construction in offshore and onshore industries. The preferability is due to many advantages, including availability, low price and high strength [26]. Carbon steel is generally composed of a minor amount of carbon ($<1.5\%$) with multiple other elements of manganese (Mn), silicon (Si), phosphorus (P), and sulfur (S). By varying the carbon content concentration, a MS can be categorized as a low ($<0.25\%$ C), medium (0.25–0.70% C), or high (0.70%–1.05% C) carbon steel. With a different composition of carbon, the steel will gain distinct mechanical characteristics, making it suitable for multiple applications [27]. For example, MS grade 1018 has an exceptional welding capability, while MS grade 1008 comes with an acceptable ductility. Although its mechanical properties can be varied, most carbon steels are exceptionally prone to corrosion when exposed to acidic, alkaline, or other corrosive environments, generally due to a passivation layer that has a low protective power [28, 29]. These issues commonly occur during industrial processing: pickling, acid cleaning, and descaling with the use of more corrosive acid such as hydrochloric acid and nitric acid. But, these methods proved to be impractical since it can promote corrosion on other exposed infrastructures.

3.1 Corrosion Mechanism of Mild Steel

The most common forms of corrosion occurring on MS are uniform corrosion and localized corrosion such as pitting and crevice corrosion. In this section, the process of uniform corrosion is described. The general mechanism of corrosion on MS, when exposed to water and oxygen, is commonly understood by the reaction of iron (Fe), as illustrated in Fig. 2 and described by multiple studies [30, 31]. The process begins when iron is oxidized at the anodic sites to form ferrous ions (Fe^{2+}) (Eq. 1) and released electrons that travel to the cathodic site through an electronic path within the metal. Upon reaching the cathodic region, these electrons consumed the water and oxygen to form hydroxide ions (OH^-) (Eq. 2). If the solution is acidic in the absence of oxygen, then the hydrogen ions (H^+) can be reduced to produce hydrogen gas (H_2) (Eq. 3). The electrochemical reaction of corrosion occurred on a metal surface because of the potential difference yielded by the metal and the surrounding electrolytes.

$$\text{Anodic reaction}: \ Fe \rightarrow Fe^{2+} + 2e^- \ \text{(oxidation of iron)} \tag{1}$$

$$\text{Cathodic reaction}: \ O_2 + 2H_2O + 4e^- \rightarrow 4OH^- \ \text{(reduction of oxygen)} \tag{2}$$

$$2H^+ + 2e^- \rightarrow H_2 \ \text{(reduction of hydrogen ions)} \tag{3}$$

The rate of corrosion is relatively understood according to Faraday's law, where it is dependent on the total flow of electrons from anode to cathode, termed as the corrosion current density i_{corr}. The corrosion current is presented in the electrolytes (water) during this cycle and flows through ionic conduction. Hence, when the conductivity of the electrolytes is increased (e.g., by adding salt), it will boost the flow of corrosion current and increase the overall rate of reaction. After the reduction occurs at the cathodic site, the formed OH^- will react with the Fe^{2+} and generate iron (II) hydroxide, $Fe(OH)_2$ (Eq. 4). The produced substance is considered as solid corrosion debris, incomplete forms of rust with a greenish color due to partial oxidation with the oxygen.

$$Fe^{2+} + 2OH^- \rightarrow Fe(OH)_2 \tag{4}$$

The corrosion debris can undergo further hydration and oxidation reaction before forming a complete corrosion product, a complex mixture known as the ferric oxide, Fe_2O_3 (Eq. 5).

$$4Fe(OH)_2 + O_2 \rightarrow 2Fe_2O_3 + 4H_2O \tag{5}$$

4 Stainless Steel (SS)

SS is a prominent alloy with various applications for construction, surgery tools, automotive, electrical machinery, and vessels [32]. It is widely known as an iron-based alloy with a higher corrosion resistance compared to most types of steel. Its composition includes chromium (Cr) as the major component with other materials of nickel (Ni), nitrogen (N), niobium (Nb), titanium (Ti), and molybdenum (Mo) [33]. As the primary material, Cr plays a crucial role in forming an

Fig. 2 Uniform corrosion of mild steel [30]

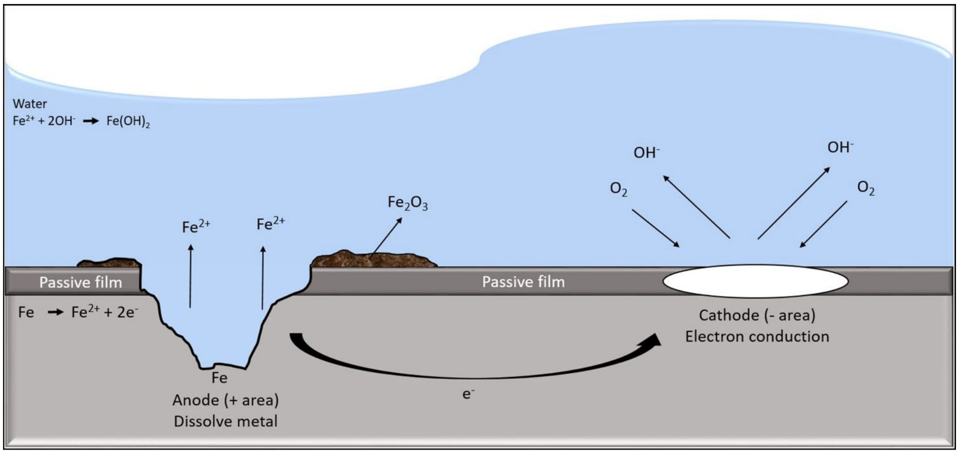

oxide film on the SS surface to prevent harmful substances from reaching the alloy during the early stage of exposure to a corrosive environment. In fact, in the presence of an oxidizing environment (therefore also in contact with the oxygen contained in the air or dissolved in water) the surface of the SS self-passivates, forming a very thin film of chromium oxide, extremely adherent and compact which protects the substrate. This invisible layer which has a thickness of a few atomic layers (2–10 nm) can regenerate itself in the case of damage, not too extensive and penetrating, reconstituting a barrier to the continuation of the attack. Essential conditions for this layer to form are the presence of a minimum content of 10.5% of Chromium (Regulation En 10,020) and the possibility of exchanging a sufficient quantity of oxygen with the surrounding environment to ensure optimal passivation conditions [34]. According to the American Institute of Steel and Iron (AISI), there are four classifications of SS, which are ferritic, martensitic, duplex, and austenitic [35]. In brief, the Cr percentage contents of ferritic, martensitic, duplex, and austenitic are 11–30%, 12–17%, 20–28%, and 16–30%, respectively. The ferritic type is known to be cheaper since it has a lower or no Ni content and can withstand high temperatures above 1000 °C. The martensitic, however, has a high carbon (C) amount that increases the steel strength and durability. As for the duplex, it is unique from the rest since the microstructure is made up of a balance combination between both ferritic and austenitic. Due to this microstructure, the duplex provides many advantages usually found in the class of ferritic and austenitic [36]. The austenitic family is the largest group of SS and can be further categorized into high-temperature austenitic grade, high-performance austenitic grade, Cr–Mn grade, Cr–Ni grade, and Cr–Ni–Mo grade [37]. The steel resistance against corrosion is good to excellent, depending on which sub-groups and the types of environment it is exposed to.

4.1 Corrosion Mechanism of Stainless Steel

The SS are commonly subjected to different forms of corrosion, such as pitting, crevice, intergranular, stress-corrosion cracking, fretting corrosion or mechanical-assisted corrosion (MAC), and uniform corrosion. During the exposure to a chloride-concentrated solution, the apparent forms of corrosion are mostly pitting and crevice corrosion. Although the forms have different names, some researchers considered that these two are the same, in which pitting is just an extended version of crevice [38]. The only main difference is that pitting corrosion does not require any prior contact with other material before it can be started. The description of the pitting mechanism is based on Fig. 3. Pitting corrosion appears as a deep, tiny hole with rust on the tip. The process begins with the oxidation of metal (Fe) naturally (Eq. 6) or due to its reaction with the acid (Eq. 7). For explanation, hydrochloric acid (HCl) is used as an example. The oxidation at the anode released electrons that can travel to the reduction site while simultaneously reacting with HCl's hydrogen ions to form hydrogen gas (Eq. 3).

$$\mathrm{Fe} \rightarrow \mathrm{Fe}^{2+} + 2\mathrm{e}^{-} \tag{6}$$

$$2\mathrm{H}^{+} + 2\mathrm{e}^{-} \rightarrow \mathrm{H}_2 \tag{7}$$

Similar to the process in Eq. 2, the released electrons, upon reaching the cathodic site, caused the formation of OH^-. The presence of OH^- combined with Fe^{2+} to produce the oxide film (Eq. 8).

$$\mathrm{Fe}^{2+} + 2\mathrm{OH}^{-} \rightarrow \mathrm{Fe(OH)}_2 \tag{8}$$

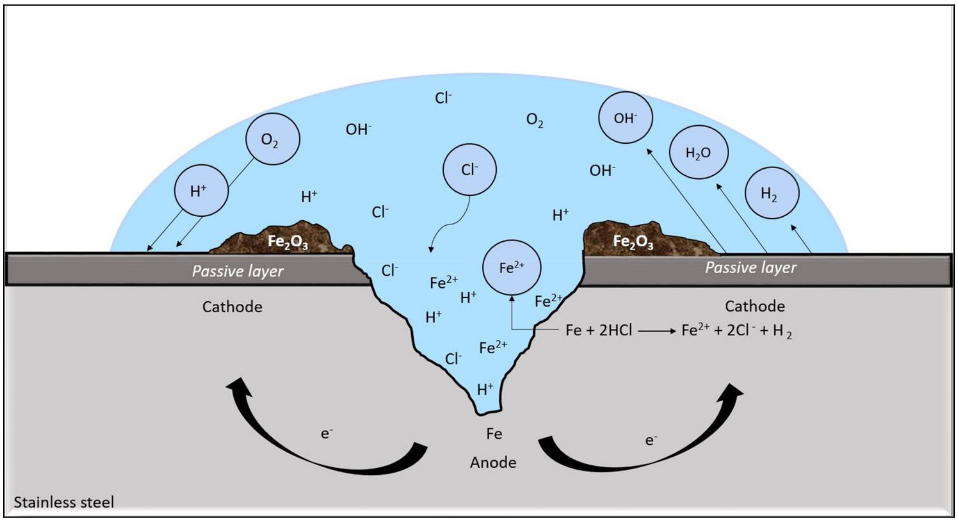

Fig. 3 Localized corrosion of pitting on stainless steel [48]

The pitting is initiated when $Fe(OH)_2$ starts to breakdown, forming a tiny hole with the shape of either hemispherical or cup, as shown in Eq. 9:

$$Fe(OH)_2 + 2Cl^- \rightarrow FeCl_2 + 2OH^- \tag{9}$$

Since the $FeCl_2$ is soluble in water, more tiny holes are formed, with each hole continues to dig down deeper until it reaches the metal surface. The formation of each hole caused corrosion to occur only on the exposed site inside the area of the breakdown. This is the primary reason why pitting corrosion is more dangerous than uniform corrosion; it is harder to detect, and from the outside, the accumulation of tiny holes makes the surface look rough, just like an ordinary form of uniform corrosion. Inside the pit, oxidation of metal continues to occur, releasing more electrons that reduce both the limited quantity of oxygen and water. When the amount of oxygen reaches zero, electrons will start to travel to the new cathodic site at the outer part of the oxide film. The depletion of oxygen also creates a potential gradient in the pit that forces corrosion to occur faster [39]. As more Fe^{2+} are accumulated, the pit becomes positively charged and attracts the negatively charged Cl^- ions from the outer part to diffuse into as a means to achieve electroneutrality [40]. Simultaneously, the Fe^{2+} can also react with H_2O, producing more H^+ (Eq. 10) that increases the acidity of the solution, rendering the pit to be more corrosive.

$$Fe^{2+} + 2H_2O \rightarrow Fe(OH)_2 + 2H^+ \tag{10}$$

In the worst-case scenario, the increase in potential and corrosivity of the solution makes the corrosion progress inside the pit to be almost unstoppable. Nonetheless, if the minimum surrounding factors during the early stage of pitting corrosion are not fulfilled, then the newly formed pits will just be instantly re-passivated [41]. On the other hand, it is also worth mentioning that when the formed oxide film on SS is disrupted by mechanical factors, it can induce MAC to occur. Similar to pitting corrosion, MAC is difficult to discern, with the surface appearing to be smooth. Hence, the damage needs to be observed through a microscope to identify the surface composed of sharp grooves and rough pits [42, 43].

In the composition of SS, the amount of chromium is a critical factor in determining the oxidation and corrosion resistance properties. When a SS starts to corrode, the process of corrosion is associated with the formation of the chromium oxide (Cr_2O_3) layer. The formation rate of Cr_2O_3 is relatively slow, but a complete form of Cr_2O_3 is capable of blocking any outward diffusion of other alloy elements and inward diffusions of corrosive agents. It is reported that the oxide films of SS are commonly made up of two layers; inner and outer layers. The reason for these circumstances is due to the simultaneous oxidizing (oxygen or hydrogen peroxide) and reducing (excess H_2) conditions that take place when a SS is subjected to an aggressive medium. Accordingly, the inner layer is composed of a fine grain oxide enriched in chromium, whereas the outer layer is constituted of a coarse layer enriched in iron. There are different types of Cr_2O_3 layers dictated by the dissimilar chromium content of a SS. For a SS with a low amount of chromium, such as stainless steel 304, the formed oxide layer is named as spinel oxide ($FeCr_2O_4$) and has a limited resistance against aggressive solutions. Two separate studies on this topic performed by Kuang et al. [44], and Ziemniak and Hanson [45] point out that the spinel oxide is a two-layer oxide film with an outer layer loosely and disorderly packed with a crystal size of 5 to 10 µm, formed through precipitation process. In contrast, the inner layer is identified to include nanocrystalline spinel oxide with a crystal size of 5 to 10 nm. Generally, as the amount of chromium is increased, the alloy will have greater resistance. For example, a SS with a chromium content above 13% displayed a much slower rate of oxidation with the inner oxide layer consisting of Cr_2O_3, $(Cr, Fe)_2O_3$, or Cr-rich $(Cr, Fe\ Mn)_3O_4$ and an outer layer composed of Fe_2O_3 [46, 47].

5 Corrosion Control Practices

Preventing corrosion is a vital maneuver to sustain the integrity and esthetic values of a structure. Since corrosion is dependent on the characteristics of both environment and metal, any changes that occur to these factors will directly impact the overall process. For example, the changes can be as simple as storing metal inside a warehouse to avoid any contact with the rain and sunlight or the procedures of polishing and grinding [49]. In short, by understanding and manipulating the surrounding environmental condition, corrosion can be reduced significantly. Generally, five corrosion prevention techniques are widely acceptable, namely cathodic protection, coatings, material selection, design selection, and corrosion inhibitors.

Cathodic protection extends the shelf life of a metallic structure by applying a regulated electrical current to polarize the metal surface and reduce the corrosion progress. It is achieved by subjugating the protected metal to function as in an electrochemical cell where it acts as a cathode in which a sacrificial metal will be reduced in its place. The two most common forms of cathodic protection are sacrificial anode cathodic protection (SACP) and impressed current cathodic protection (ICCP) [50–53]. The second alternative for corrosion protection is coating. A coating is considered the first line of defence that separates a metal from its surrounding. In today’s world, the coating is present virtually on almost any human-made structure. Due to the numerous types of coatings available on the market, a selection of coating is generally determined by the environmental condition (such as highly corrosive, moderately corrosive, and lightly corrosive) or types of polymer used. Although coatings seem like an ideal protection method, two limiting factors are the cost of materials and the extensive requirement of surface preparation. It is also necessary to consider that when we talk about coating, we really mean a "coating system" that consists of several layers, sometimes even of different types (e.g., gel-coat, primer, top coat, etc.) [54–59]. In contrast, material selection occurs during an earlier phase compared to the other prevention methods. It highlights the selection of materials which has the highest compatibility with the environment. Technically, for most industries, the resistant alloy would be the optimum choice [60]. However, severe problems with resistant alloys are the high initial cost, difficulty to manufacture, and, most importantly, inability to meet the engineering demand. Due to these disadvantages, material selection as the only prevention method on any structure is not practical [61]. Design decreases the corrosion by avoiding a particular structure from trapping dust and moisture for an extended period while ensuring an accessible path for regular maintenance to be conducted regularly. Finally, among these prevention techniques, the corrosion inhibitor is appraised as the cheapest, sensible, eco-friendly, and convenient method to manage corrosion in an aqueous environment [62–64].

6 Corrosion Inhibitors (CI)

Corrosion inhibitor is a chemical substance that reduces the corrosion rate when present in a corrosive system at suitable concentrations, without significantly changing the corrosive environment (ISO). The working mechanism of organic and inorganic corrosion inhibitors differs through their inhibitive action, where an organic inhibitor lowers the corrosion rate by the adsorption process and the inorganic inhibitor by reacting with the formed anodic and cathodic sites [65, 66]. Figure 4 shows the general classification for organic and inorganic corrosion inhibitors [67]. The classification of inhibitors is also discussed based on their inhibitive mechanism such as anodic and cathodic inhibitive actions. Concerning the anodic corrosion inhibitor, it can be further divided into oxidizing and non-oxidizing anions. For oxidizing anions, the inhibitive action is by promoting the formation of an oxide layer over the metal surface in the absence of oxygen. Contrarily, the non-oxidizing anions reduce the corrosion rate by passivating the metal from initiating the redox reaction in the presence of oxygen. As for the cathodic inhibitor, it works through a precipitation process on the cathodic site causing the rate of hydrogen evolution to diminish and slow down the occurrence of corrosion [68]. Moreover, it can inhibit corrosion as an oxygen scavenger or cathodic poison by reducing the number of corrosive agents present in the environment. Cathodic inhibitor

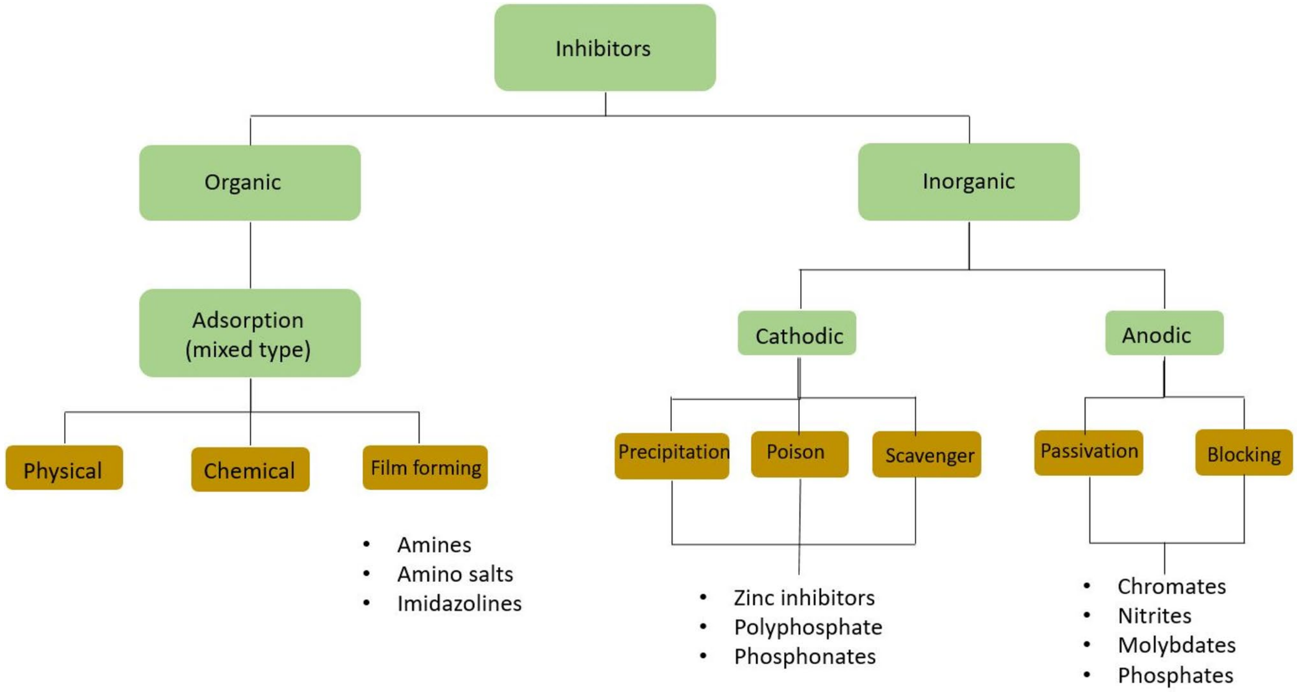

Fig. 4 General classifications of corrosion inhibitors

generally provides an optimum inhibition when deployed in neutral and alkaline solutions by performing a cathodic-oxygen reduction process. Several critical parameters need to be taken into consideration before an inhibitor is selected, which are (i) the inhibitor solubility in the selected medium, (ii) compatibility with the environment, (iii) stability with pH and temperature variation, (iv) cost, and (v) efficiency. Throughout the years, a considerable amount of effort in finding the best organic corrosion inhibitor for various corrosive media has been conducted compared to the inorganic CI. This preferability is because organic inhibitors have excellent solubility in water, lower toxicity, and are relatively inexpensive. Furthermore, since the increase of awareness for "greener" products in society to limit the discharge of contaminated substances to the environment has skyrocketed, more study has shifted towards developing organic and eco-friendly (green-based) inhibitors [69]. The organic CI inhibits corrosion through the adsorption process that is divided into three different pathways of physical, chemical, and film-forming.

An organic CI is commonly identified by the presence of heteroatom in its structure. These heteroatoms include oxygen (O), nitrogen (N), sulfur (S), and phosphorus (P), with the properties of high basicity and electron density [70]. Although many studies centered their discussion on the effects of heteroatom, the key player in combating corrosion is the functional group. Hence, each organic inhibitor must possess at least one functional group that provides an overall adsorption strength through its charge [71]. Multiple works of literature also reveal that the presence of heteroatom with the characteristics of low electronegativity and high polarizability gives the functional groups its ability to cover a larger surface area and easier electron transfer process [72, 73]. According to the previous studies, organic inhibitors are known to initiate their protective mechanism by displacing the electrolyte's molecules and adsorbing to the metal surface, resulting in a monomolecular barrier-like structure that blocks the metal from having direct contact with the corrosive agents. In general, the inhibition efficiency of organic inhibitors is based on the heteroatoms with a sequence of $O < N < S < P$. The performance of organic inhibitors is also attributed to (i) chain length, (ii) size of the inhibitor molecules, (iii) cross-linkage formation, (iv) solubility in electrolytes, and (v) types of bonding. The most explored chemical groups of organic inhibitors are polymers [74, 75], fatty amides [76–79], azoles [80–82], pyridines [83, 84], and imidazolines [85, 86].

The importance of organic inhibitors becomes apparent when discussed in its usage for acid cleaning procedures on an industrial scale. At the initial phase of the cleaning process, a metal (e.g., iron, magnesium, zinc, and copper) is exposed to acid to remove unwanted solids formed on its surface. However, the process causes the metal to undergo a severe corrosion reaction, resulting in a considerable loss of some parts. As such, to counter this problem, an organic inhibitor is usually included in the cleaning process to enhance the metal resistance towards the corrosive agents and reduce the degradation that may occur [68]. Besides the acid, the inhibitor employment against salt solution is also frequent. Infrastructure like pipelines, desalination plants, vessels and pulps, oil storage tanks, and ballast tanks require the inhibitor to increase their shelf life [87].

7 Organic CI in Corrosive Solutions

7.1 Organic Corrosion Inhibitors in Salt Solution

Wang et al. [88] studied the inhibition efficiency of an internal blending organic CI in chloride-contaminated simulated concrete pore solution for the protection of MS using the weight loss (WL) test, electrochemical impedance spectroscopy (EIS), and scanning electron microscope (SEM). The inhibition effectiveness improved with increasing concentration, and the highest efficiencies 88.73% (WL) and 89.08% (EIS) were recorded at 4% of inhibitor concentration. Decreasing the value of the pH medium also revealed a significant drop in the impedance arc radius, indicating a faster corrosion rate occurred in a lower pH condition. Based on the surface analysis, the authors reported that an absence of inhibitor caused severe pitting corrosion with distinct rough layers on the steel surface. In contrast, the presence of an inhibitor was observed to form a compact and uniform monomolecular film on the steel surface, preventing it from initiating any visible corrosion reaction.

Deyab and Guibal [89] tested the *Taraxacum officinale* extract (TOE) as a corrosion inhibitor for cooling systems in desalination plants. The evaluation was carried out on carbon steels in a seawater environment and characterized using WL, EIS, and potentiodynamic polarization (PP). An increase in the TOE concentration corresponded with the increase in efficiency. The results from WL confirmed that the highest inhibition efficiency of TOE 94% was obtained at 400 mgL^{-1} of inhibitor concentration after 7 days of immersion, and an extended testing period beyond 24 days revealed an efficiency of 91%. These findings also agree with the results of EIS and PP, in which the optimum TOE concentration produced 90.4% and 88.2% efficiencies, respectively, when assessed at 298 K, significantly higher than other concentrations (100, 200, and 300 mgL^{-1}). The author summarized the inhibitive actions of extract to work predominantly as an anodic inhibitor. Comparative research by Fouda et al. [90] explored the inhibition effects of *Medicago sativa* (Alfafa) on MS in a solution containing 3.5% NaCl and 16 ppm of sodium sulfide (Na_2S) using the characterizations of WL, EIS, and PP. As the concentration of

Alfafa increased, the inhibition efficiency also increased. The optimum concentration of Alfafa at 300 ppm yields efficiencies of 74.5%, 92.7%, and 98.5% for WL, EIS, and PP, respectively, after 120 min of immersion at 25 °C. The effects of temperature are observed using WL from 25 to 45 °C, in which a decreased inhibition efficiency of optimum Alfafa was recorded from 74.5 to 69.6%, respectively. The author concluded that the adsorption of Alfafa molecules followed the Temkin isotherm, and its inhibitive action is a mixed-type. The fruit shell extract of *Juglans regia* was researched by Haddadi et al. [91] as an organic corrosion inhibitor on MS in 3.5% NaCl solution through both means of computational and experimental. The theoretical characterizations performed were molecular dynamics, Monte Carlo (MC), and quantum mechanics computation of density functional theory (DFT). Meanwhile, the experimental analysis was EIS, PP, and field emission scanning electron microscope (FESEM) coupled with an energy-dispersive X-ray (EDX). The theoretical study points out the adsorption affinity between the inhibitor molecules and the surface of MS. According to the author, out of all species presented, myricetins provide the highest adsorption level as suggested by the molecular simulator, with its lowest computed negative energies being − 279.63 kcal/mol. Other theoretical analyses also proposed that the reactive sites of all phenolic-based compounds have excellent affinity for the adsorption process through the donor–acceptor interaction. In regard to the experimental examination, the best efficiency obtained was 94.2% for the concentration of 1000 ppm after 48 h of the exposure period. The extract was also discovered to be a mixed-type inhibitor since it retards both anodic and cathodic reactions. Additionally, the protective function of the extract is evident based on the surface study, where a uniform layer of inhibitor was found to cover the metal surface, and fewer corrosion products were detected. Several previous studies are also in agreement with the findings using different plant extracts of *Allium sativum*, *Ferula asafoetida*, *Leucaena leucocephala*, *Olea sp*., and *Andrographis paniculata* [92–95].

In another study, Loto et al. [96] examined the different concentrations of calcium gluconate (CGN) as a non-toxic CI in artificial seawater (3.5% NaCl) for MS protection using PP, open circuit potential (OCP), WL, and optical microscopy. The CGN was confirmed as a mixed-type inhibitor with a dominant anodic. The inhibitor with an optimum concentration of 1.75% yields an efficiency of 85.14% and 97.87% for PP and WL studies, respectively. The optical microscopy revealed that chloride ions aggressively promote pits on the MS surface via an autocatalytic oxidation process in the absence of an inhibitor. In the presence of CGN, the surface displayed a lower morphological degradation and a complete absence of pits. They concluded that the excellent performance of CGN is due to its strong attraction and coordinated reaction onto the MS surface.

The inhibition properties of amino-based protic ionic liquids such as N-methyl-2-hydroxyethylamine (M-2HEAOL) and bis-2-hydroxyethylamine (B-HEAOL) oleate were analyzed for MS (AISI 1020) protection in a naturally aerated chloride solution (0.01 mol/L), using OCP, PP, SEM, and optical interferometry [97]. Besides, both inhibitors were identified as a mixed-type with a predominant anodic inhibition effect and produced a similar efficiency of 97% according to the PP analysis when used at 5 mmol/L concentration. The retardation is through an adsorption reaction (followed Langmuir isotherm) of physisorption and chemisorption mechanisms. The presence of M-2HEAOL and B-HEAOL also modified the hydrophilic surface property to hydrophobic, and this is evident from the surface analysis, which displayed imperceptible corrosion marks, even though the study was conducted in an accelerated condition.

Another exciting research by Moradi et al. [98] used the *Pseudoalteromonas piscicida* (*P. piscicida*) to inhibit corrosion through the formation of a biofilm on A36 MS immersed in artificial seawater for 14 days. The immersion was conducted in two different hydrodynamic conditions of orbital shaking incubator and flat plate bioreactor, in which characterizations included were EIS, PP, FESEM, and confocal laser scanning microscope (CLSM). The polarization study confirmed the inhibitory effect of *P. piscicida* in the first week of exposure, while the lowest corrosion rates of 0.009 mpy and 0.027 mpy were recorded after 14 days for orbital shaking conditions and flat plate bioreactor, respectively. As for the EIS evaluation, although an identical result was obtained for the orbital shaking condition after 14 days of immersion ($R_{ct} = 70{,}250\ \Omega\ cm^2$), a different finding was displayed for flat-plate bioreactor condition, where an increase of R_{ct} was only recorded for the first week, and an increase of exposure to 2 weeks reduced it to $9854\ \Omega\ cm^2$. According to the author, the difference is due to the formation of heterogeneous biofilm beyond a week of exposure in the flat plate bioreactor, causing a severe corrosion reaction on MS. The surface analysis revealed a uniform and compact multilayer of biofilm on the steel surface under the orbital shaking condition. In contrast, the biofilms formed in flat plate bioreactor conditions were heterogeneous, mushroom-like with various sizes and open gaps. The finding, thus, supported the data recorded in the EIS study.

A novel application of gemini surfactants prepared by the reaction of Bis[2-(*N*, *N*-dimethylamino)ethyl] ether and chloroesters, such as N2OE8 (3-oxa-1,5-pentamethylene–bis(*N*-octyl-2-chloroacteate-*N*, *N*-dimethylammonium chloride) and N2OE10 (3-oxa-1,5-pentamethylene–bis(*N*-decyl-2-chloroacteate-*N*, *N*-dimethylammonium chloride) were evaluated by Pakiet and coworkers [99] on MS in a solution of 50 mM NaCl, using both experimental and theoretical studies of DFT, PP, EIS, and linear polarization resistance (LPR). The theoretical analysis implied that both inhibitor's structures are thermodynamically stable and adsorb on the metal surface via the physisorption mechanism. Furthermore, the N2OE8 showed a more exceptional softness, σ than N2OE10, indicating a higher tendency for donor–acceptor interaction and possibly a more reliable bond formation. In regard to the experimental analysis, the addition of inhibitors shifted the potential towards more positive regions and acted as a mixed-type inhibitor with a predominant anodic effect. The highest efficiencies obtained according to the PP analysis were 79% for 8.5 mM of N2OE8 and 62% for 1.7 mM of N2OE10. These results are also in agreement with both EIS and LPR characterizations, in which the N2OE8 exhibited a higher efficiency than N2OE10, even when CMC (Critical Micelle Concentration) parameter is included. Further comparison between these gemini surfactants inhibitors with a commercial 1H-benzotriazole displayed a significant output, for which both surfactants were shown to have higher protective capabilities after an extended immersion test.

Wang et al. [100] elucidate the inhibitive effects of a modified chitosan-oligosaccharide (MCO) at different concentrations and sodium silicate (SA) at a fixed concentration for MS in 3.5 wt% of NaCl solution, using WL, EIS, PP, and SEM/EDX analysis. The test was conducted for a maximum of 48 h, with the effects of temperatures were also included. Based on the WL study at 300 K, the MCO at 700 ppm concentration gave the highest efficiency of 80.78%, and SA at 350 ppm concentration yielded an efficiency of 84.70%. Similar findings were also recorded by EIS and PP studies, where both MCO and SA, at an optimum concentration, have retained a similar trend with the efficiencies of 81.42% and 85.64% for EIS, and 81.45% and 82.60% for PP, respectively. The inhibitive mechanism of the inhibitors was also identified as a mixed-type. Besides, the author discussed the synergistic effects by combining both inhibitors at a fixed concentration of 350 ppm. The efficiency outputs of this combination were 94.31%, 92.95%, and 96.71% for the characterizations of WL, EIS, and PP, respectively. As for the surface morphology study, although the presence of inhibitors, as an individual, has significantly reduced the corrosion, the presence of localized attacks was still discernible. In comparison, the mixed inhibitors of both MCO and SA provided a much more superior inhibitive action, in which the displayed steel surface was markedly smooth.

Somers et al. investigated the inhibition efficiency and synergistic effects of a new and environmentally friendly rare earth (RE) 3-(4-methylbenzoyl)propanoate (mbp) carboxylate (RE = Lanthanum (La), Cerium (Ce), Neodymium (Nd), and Yttrium (Y)) as corrosion inhibitors tested on MS immersed in 0.01 M NaCl. After 30 min of immersion in 0.25 mM, all the compounds started to show some inhibition effect. From the electrochemical measurements, $Y(mbp)_3$ showed the highest corrosion efficiency (IE) at nearly 90%, while $La(mpb)_3$ has the lowest inhibition efficiency with the concentration of 0.25 mM. From the polarization study, the effect of $Y(mbp)_3$ on i_{corr} was greater than others, demonstrating the synergistic effects between RE and mbp ligand. Furthermore, based on the SEM/EDX result, the highest level of RE observed was on the exposed samples of $Y(mbp)_3$. After 6 h of immersion in NaCl, the level of effectiveness is concluded as $Y(mbp)_3 > Nd(mbp)_3 > Ce(mbp)_3 > La(mbp)_3$ [101]. Similarly, Peng et al. [102] also studied rare-earth 3-(4-methylbenzoyl)-propanoate compounds as CI for AS1020 MS in NaCl solutions using PP and EIS techniques. The three types of CI employed were (La(4-OHcin)$_3$, $La(mbp)_3$, and $Y(mbp)_3$). In PP results, $Y(mbp)_3$ caused a shift of corrosion potential (E_{corr}) towards more positive potential with the highest IE of 97%, in comparison to La(4-OHcin)$_3$ and $La(mbp)_3$ with the IE of 93% and 82%, respectively. The findings indicate that both 97% and 93% IE demonstrated a better inhibition performance in 0.25 mM concentration. To conclude, at the concentration of 0.25 mM, the $Y(mbp)_3$ compound achieved the highest efficiency in both short (30 min) and the extended (24 h) immersion time, indicating that it could be a promising corrosion inhibitor for MS in aqueous salt solutions.

Talebian et al. [103] evaluated the inhibitive effect of sodium (E)-4-(4-nitrobenzylideneamino) benzoate (SNBB) on three different types of metals which are pure iron, copper, and low alloy carbon steel (grade F111) in a neutral 10 mM NaCl solution. Three different concentrations (1 mM, 5 mM, and 10 mM) of SNBB and control samples were tested at 25 °C. The IE keeps increasing as the concentration increases, in which the highest recorded IE was 91% with 10 mM for F111 steel, while 81% of IE was measured for Fe. From PP analysis, pure iron and F111 steel displayed a remarkable decrease in corrosion rate, except copper. Additionally, the use of SNBB on iron and F111 was found to obey the Langmuir adsorption isotherm. The subsequent thermodynamic analysis revealed that the adsorption mode was both physisorption and chemisorption. The summary of different types of organic corrosion inhibitors in the salt solution, as discussed in the section, is presented in Fig. 5.

7.2 Organic Corrosion Inhibitors in Acidic Solution

Dehghani et al. [104] explored the aqueous Chinese gooseberry fruit shell (CGFS) as a green and cheap corrosion inhibitor for MS in HCl solution. Several concentrations of CGFS (0 ppm, 400 ppm, 600 ppm, 800 ppm, and 1000 ppm) were used in the study. According to EIS, after 2.5 h of immersion, the highest recorded IE was 92% when using 1000 ppm concentration, while 400 ppm gave the lowest IE at 85.8%. Correspondingly, with the increase of CGFS

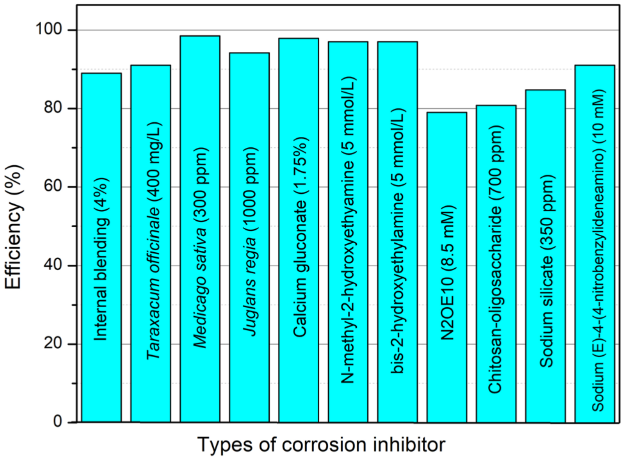

Fig. 5 Summary of organic corrosion inhibitors in the salt solution

extract concentration, the IE and resistance values also increased. The improved resistance is evident from the surface analysis that showed a steady formation of a protective layer on MS, causing the surface to become smoother. Similar findings were displayed in polarization measurement, in which i_{corr} and E_{corr} parameters decreased as the CGFS concentration increased. Also, the inhibition of CGFS was found to be a mixed type with a predominant cathodic suppression. Based on the wettability evaluation, the contact angle of the water droplet continues to increase with concentration, and the highest angle was 79° at 1000 ppm concentration. The DFT theoretical analysis also highlighted that the flat structure of N-containing compounds provides more inhibiting strength than sucrose and maltose due to its oxygenated polar centers. Fernandes et al. [105] discussed *Ircinia strobilina* crude extract (ISCE) as a corrosion inhibitor for MS in HCl medium. The corrosion behavior was analyzed using WL, PP, and EIS. In this study, different concentrations of ISCE (0.5 gL^{-1}, 1.0 gL^{-1}, 1.5 gL^{-1}, and 2.0 gL^{-1}) were inserted in the 1 $molL^{-1}$ of HCl. From the WL study, the increased concentration of ISCE was found to increase the surface coverage of the passive film. The maximum value of IE 82.3% was achieved at 2 gL^{-1} inhibitor concentration. Meanwhile, the lowest IE was 49.5% by 0.5 gL^{-1} concentration. According to PP evaluation, with the addition of inhibitor in HCl solution, both anodic and cathodic parts of the curve displayed decreasing values of i_{corr}, signifying a lower corrosion rate. The shift in E_{corr} from 20 to 51 mV towards more negative potential region is below 85 mV, proving that ISCE is a mixed-type inhibitor. Consequently, Divya et al. [106] also performed a similar analysis using the flower extract of *Tithonia diversifolia* (TDFE). The study employed conventional characterizations of WL, EIS, and PP to evaluate the effects of TDFE inhibitor on the protection of MS. An initial analysis by exposing the MS in HCl at 30 °C displayed an optimum efficiency of 94.55% at 0.7% concentration. Next, a further evaluation by varying the immersion period and temperature was conducted. The prolonged immersion period for 24 h provided stable data on 0.7% concentration, where for each subsequent 1, 3, 6, and 24 h, the concentration showed constant efficiencies above 90%. As for the temperature variation, with increasing values from 305 to 355 K, the TDFE of 0.7% concentration gave the highest IE until 355 K, where it drops a bit lower than other concentrations at 91.76%. In addition, several recent studies using the plant extracts of *Thymus algeriensis* [107], *Urtica dioica* [108], lychee fruits [109], *Glycyrrhiza glabra* [110], and coffee husk [111] also displayed promising results for the same protection purpose.

In another research, Singh et al. [112] investigated the potential of a modified expired drug Dapsone and its resulting product (Schiff base (SB)) as a corrosion inhibitor on MS sheet in H_2SO_4 solution. The study deployed four types of inhibitors without (SB-1 and SB-2) and with potassium iodide, KI (SB-1 + KI and SB-2 + KI) at different concentrations ranging from 0.0548 to 0.219 mM to evaluate its synergistic effects. Several characterizations included are WL, EIS, PP, SEM, atomic force microscopy (AFM), and DFT. The result from WL measurement indicated that the individual usage of SB-1 and SB-2 gave the IE of 95.67% and 94.23% at 0.219 mM concentration, respectively. Interestingly, with the addition of KI, a positive synergistic impact was observed where both SB-1 + KI and SB-2 + KI displayed a higher IE at 99.03% and 97.98%, respectively. The findings were supported by EIS analysis, in which the IE for SB-1 and SB-2 reached maximum values of 95.12% and 92.53%, respectively. Correspondingly, both SB-1 + KI and SB-2 + KI reached maximum values of IE 98.70% and 97.41%, respectively, at the same concentration. The polarization investigation revealed that the inhibitors act as mixed-type inhibitors with predominant cathodic action. Following the DFT calculation, SB-1 showed a higher proton affinity than SB-2, indicating a higher reactivity and better adsorption ability, which supported the experimental results. Also, the surface observation of SEM and AFM illustrated a smooth surface for the immersed MS with the inhibitors.

Espinoza et al. [65] reported the corrosion inhibition of MS (API 5L X52) using fluconazole (1) and its fragments (1,2,3-triazole (2) and 1-bromo-2,4-difluorobenzene (3)) in the 1 M HCl solution. The experimental evaluations involved were EIS, PP, and SEM, while the theoretical study was DFT. The electrochemical measurements displayed a steady increase in IE as the concentration of fluconazole was increased. The best performance was recorded at the highest concentration of 200 ppm, with 90.6% efficiency. In contrast, the highest IE recorded for fragments 2 and 3 were slightly lower than fluconazole at an average of 83% IE (at 30 ppm concentration) and 80% (at all concentrations). The isotherm behavior was also different where fluconazole followed Langmuir mode of chemisorption and physisorption process, whereas 2 and 3 a physisorption mode. A prolonged investigation on fluconazole (100 ppm) efficiency was discovered to be limited up until 168 h of immersion, in which the IE started to decrease below 22% after 336 h. The DFT evaluation suggests that fluconazole has the most prominent energy of the highest of occupied molecular orbital, E_{HOMO} at -6.516 eV, indicating an easier electrons donation during the bonding formation process between inhibitors and the steel. The condition provides a faster adsorption process for the inhibitors to cover the steel surface and prevent the penetration of corrosive substances. Conclusively, both experimental and theoretical analyses are in agreement.

Verma et. al. [113] performed an experimental and theoretical assessment on the inhibitive action of three choline-based ionic liquids, specifically 2-hydroxyethyl-trimethyl-ammonium chloride [Chl][Cl], 2-hydroxyethyl-trimethyl-ammonium iodide [Chl][l], and 2-hydroxyethyl-trimethyl-ammonium acetate [Chl][Ac]. The experiments were conducted on MS in HCl medium with multiple characterizations of WL, EIS, OCP, PP, and SEM/EDX. As for the theoretical study, the DFT calculation and MC were employed. The WL demonstrated that all inhibitors showed an increase in efficiency with the increase of concentration. On average, the order of lowest to highest efficiencies are [Chl][Cl] < [Chl][l] < [Chl][Ac] at 92.04%, 96.02%, and 96.59%, respectively, at the same concentration of 17.91×10^{-4} M. Furthermore, the electrochemical measurements of EIS, PP, and OCP also supported the results from the WL analysis with the inhibitors were determined to act as a mixed-type. Based on DFT simulation, the inhibitors were proposed to form the bonds with MS through donor–acceptor interaction, where the electron donor is the anionic component, and the acceptor is the cationic component. Also, the MC analysis suggests that the efficiency of inhibitors primarily depends on the characteristics of anionic moieties to enhance the spontaneous adsorption process. The outputs of DFT and MC support the experimental findings with a similar order of efficiencies by the inhibitors.

Evaluation of chitosan as a green inhibitor was investigated by Rabizadeh & Khameneh [114] using the approach of WL, EIS, PP, thermodynamic, adsorption isotherm, and AFM/EDX. The experiment was conducted on MS in HCl solution by varying the inhibitor concentrations from 0.3 to 1.8 mM. An increase in concentration produced a higher IE up to 92.1% for 1.8 mM in the WL analysis, after 24 h of immersion at 298 K. A further increase in the temperature to 328 K, however, caused an adverse effect where the performance of 1.8 mM of chitosan rapidly reduced to 67%. The adsorption mechanism followed the Langmuir isotherm, a typical standard by many organic inhibitors. Based on the electrochemical findings, chitosan was determined to be a mixed-type inhibitor with a predominant anodic tendency. Also, compared to the blank sample, 1.8 mM of chitosan managed to significantly increase the resistance values from 88.55 to 973.9 Ω cm^2. The surface characterization of AFM showed that the MS immersed with an optimum chitosan concentration yielded a smooth surface, almost similar to the condition of a freshly polished MS. The data provided by EDS also supported the analysis where the oxygen intensity was recorded to drop sharply with no chlorine peak, implying that less corrosion process has occurred. The summary of organic corrosion inhibitors in acidic solution, as discussed in the section, is presented in Fig. 6.

8 Mechanism of Organic CI

From a careful analysis of previous literature, the primary mechanism of organic inhibitors in inhibiting corrosion on a metal surface is through the donor–acceptor interaction or adsorption. Although there are other models presented to describe the working principles of organic inhibitors, the model of adsorption is the most widely accepted as of now [115–119]. According to this model, the inhibiting process is initiated by a displacement reaction where the inhibitors will remove or displace the adsorbed water molecules presented on the metal surface, as shown in Eq. 11. The reaction displayed is not purely considered as physical or chemical; it can be both with a dominant action of chemical adsorption. In short, physical interaction is based on a charge differential between the inhibitor and metal surface, while a chemical interaction is associated with the mentioned donor–acceptor interaction.

$$\mathrm{Org}_{(sol)} + \alpha\mathrm{H_2O}_{(ads)} \leftrightarrow \mathrm{Org}_{(ads)} + \alpha\mathrm{H_2O}_{(sol)} \tag{11}$$

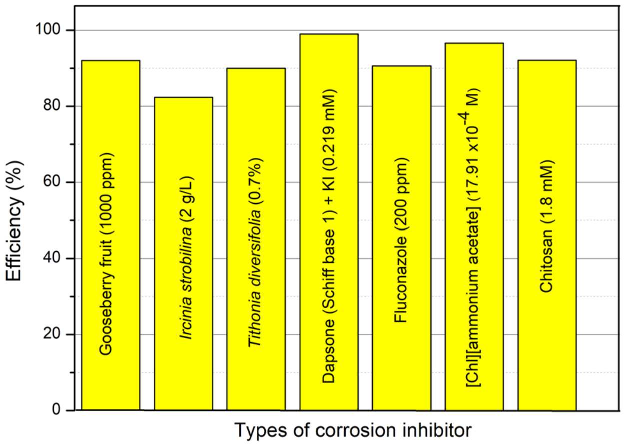

Fig. 6 Summary of organic corrosion inhibitors in acidic solution

Most of the reported studies showed that the heteroatom within the side chain or aliphatic ring(s) is responsible for establishing bonding with the metal surface. There are four methods of adsorption performed by the inhibitors, which are derived from both physical and chemical reactions, i.e., electrostatic or charge differential adsorption (physisorption), back bonding (retro-donation), chemisorption, and organometallic complex reaction [120, 121].

To describe the adsorption process, consider the following description based on Fig. 2. When an inhibitor is placed in a container containing a corrosive acidic (e.g., HCl and H_2SO_4) solution, the heteroatoms with lone pair electrons will undergo a protonation reaction causing it to be in the cationic forms. Simultaneously, the metal surface exposed to acid also undergoes a rapid corrosion process, changing its neutral condition to be positively charged. This state of the metal surface attracts the surrounding negatively charged ions formed from the acid, such as chloride and sulfate ions. These negative ions then adsorb on the metal surface and change its state from positively charged to negatively charged. As the protonated inhibitors have an opposite charge, they will be attracted to the surface due to the electrostatic reaction and begin to adsorb and form layers of monomolecular films [122–124]. Although the formed films can reduce corrosion, some parts of the metal surface are still subjected to degradation. This degradation released electrons consumed by protonated hydrogen and released hydrogen gas that neutralized the protonated heteroatoms of inhibitors. In its neutral form, the heteroatom with non-bonded electron pairs will transfer its electrons to the vacant d-orbital of the metal surface, thus establishing a chemisorption reaction. As time passes, the number of electrons transferred onto the metal surface will accumulate beyond the surface capacity and induce the inter-electronic repulsion. When this repulsion occurs, the accumulated electrons in the d-orbital of the metal surface will reverse transfer to the empty molecular orbitals of the inhibitor. Also, the reverse reaction depends on the number of electrons gathered on the surface, whereby as the number of electrons increase, a more significant reverse reaction or retro-donation can be observed. In essence, the formation of protective films by the inhibitors on any metallic surface that is immersed in acidic media can be summarized through the physisorption and chemisorption mechanisms. Moreover, the inhibitors with a molecular structure containing releasing substituents like $–CH_3$, $–NH_2$, –OH, and $–OCH_3$ have been reported to have a higher inhibitive efficiency than the inhibitors with a molecular structure containing withdrawing substituents like –COOH, $–NO_2$, and –CN [68, 125].

Additionally, besides the protection provided by the hydrophobicity of adsorbed film, the inhibition of organic inhibitors is also explained as a mixed-type, where it acts as through both anodic and cathodic inhibition action. An anodic inhibitor has two inhibitive mechanisms, which are passivation reaction and blocking of the anodic process. The passivation works by shifting the corrosion potential of the surface towards a more positive or noble region (more than 85 mV), thus passivating it from instigating anodic reaction. In comparison, the blocking action began with the inhibitors reacting with the formed corrosion product (e.g., ferrous hydroxide) and formed an insoluble film that covers the surface from being exposed to corrosive agents. The main issue of anodic inhibition is its dependency on the right number of inhibitors present in the solution. If the amount is low, some of the surface areas will not be covered by the insoluble formed film, and this condition is worse than without inhibitors since localized corrosion such as pitting and crevice corrosion can be initiated on that sites. Hence, it is of utmost importance to ensure the number of inhibitors is always high enough in the medium [126]. As for the cathodic inhibitors, the inhibition mechanisms are primarily associated with three processes of cathodic precipitation, cathodic poison, and oxygen scavenger. Generally, the cathodic precipitation works by reducing the amount of corrosive or reducing agents from diffusing into the cathodic area and completes the corrosion process. Its presence shifts the corrosion potential towards a more negative region (more than 85 mV) and critically lowers the cathodic current density. Contrarily, the cathodic poison retards corrosion by disrupting the cathodic reduction process that must be balanced with the anodic oxidation process. The inhibition is achieved by reducing both O_2 and H_2O from reacting with the electrons from the oxidation sites. Although this mechanism is very efficient, it can also prevent the hydrogen ions from forming into the hydrogen gas, leaving it to react with the metal. After a prolonged reaction with the metal, the situation can lead to the formation of hydrogen sulfide, a harmful substance with the properties of highly poisonous, corrosive, and flammable [127]. A simple process of cathodic poison by the reactions of Cr is as follows [128]:

$$3O_2 + 2Cr_2O_3 \rightarrow 4CrO_3 \tag{12}$$

$$O_2 + 4H_2O + 2Cr_2O_3 \rightarrow 4CrO(OH)_2 \tag{13}$$

$$3O_2 + 4H_2O + 2Cr_2O_3 \rightarrow 4CrO_2(OH)_2 \tag{14}$$

On the other hand, an oxygen scavenger or oxygen absorber functions to partially or entirely remove any presence of oxygen inside a medium. Its usage is mostly found in oil and gas production installations or seawater injection systems. The application also depends on several factors, including the amount of oxygen present in the fluid, environmental condition, the passivity of metal to be protected, and expense commitment. The main advantage of an oxygen scavenger is the formation of the harmless byproduct when completing the inhibition process [129].

9 Conclusions

Corrosion inhibitors to provide essential protection on tools and equipment in the industry sector during the process involving corrosive liquids are essential to regulate and reduce the degradation process. The mechanisms of uniform corrosion, localized corrosion, inhibitors working principles, chemistry, and recent developments are summarized. Since most conventional inorganic and synthetic inhibitors have negatively impacted the environment, the relevant trend of developing corrosion inhibitors is based upon the two primary properties of non-toxic and eco-friendly. Hence, with these aims, an in-depth understanding concerning the application of organic inhibitors has been consolidated in this article. The following suggestion deserved more awareness for future inhibitors exploration:

1. There is an increase in the demand for novel water-based inhibitors with better corrosion protection due to the present products can only function efficiently in a short duration.
2. More experimental analyses on the synergistic effects between inhibitors should be investigated.
3. The usage of plant extract and bio-based inhibitors showed promising results. Hence, in consideration of the current trend, the development of a better treatment method is necessary.
4. The studies on expired drugs as CI should be further investigated as it will resolve the issue of expensive initial cost.
5. More studies to investigate the eco-friendly materials possibly produced from modern approaches such as solid-phase syntheses, mechanochemical mixing, and ultrasound irradiations can be examined
6. The role of nanoparticles as corrosion inhibitors has not been profoundly analyzed and requires further research.

Acknowledgements Sincere gratitude to the Universiti Malaysia Terengganu for providing the necessary tools to complete the review.

Funding This research was funded by the Ministry of Higher Education (Malaysia) through the Fundamental Research Grant Scheme (Award no. FRGS/1/2018/WAB09/UMT/02/2, Vot no. 59537).

Declarations

Conflict of interest On behalf of all authors, the corresponding author claims no conflict of interest.

References

1. Tamalmani K, Husin H (2020) Review on corrosion inhibitors for oil and gas corrosion issues. Appl Sci. https://doi.org/10.3390/app10103389
2. Xiaofei Z, Tao M, Xiaochun H, Jinde Z, Xiaoyi W, Sixian R (2020) Flow accelerated naphthenic acid corrosion during high acid crude oil refining. Eng Fail Anal. https://doi.org/10.1016/j.engfailanal.2020.104802
3. Zhang Q, Zheng M, Huang Y, Kunte HJ, Wang X, Liu Y, Zheng C (2019) Long term corrosion estimation of carbon steel, titanium and its alloy in backfill material of compacted bentonite for nuclear waste repository. Sci Rep. https://doi.org/10.1038/s41598-019-39751-9
4. Ganjeh M, Jafari SM, Amanjani M, Katouzian I (2017) Modeling corrosion trends in tin-free steel and tinplate cans containing tomato paste via adaptive-network-based fuzzy inference system. J Food Process Eng. https://doi.org/10.1111/jfpe.12580
5. Rajput A, Park JH, Hwan Noh S, Kee Paik J (2020) Fresh and sea water immersion corrosion testing on marine structural steel at low temperature. Ships Offshore Struct. https://doi.org/10.1080/17445302.2019.1664128
6. Wu J, Zhang W, Chai K, Yu A (2020) Corrosion behavior of AISI 1045 steel in seawater in the presence of *Flavobacterium sp*. Front Microbiol. https://doi.org/10.3389/fmicb.2020.00303
7. Askari M, Aliofkhazraei M, Afroukhteh S (2019) A comprehensive review on internal corrosion and cracking of oil and gas pipelines. J Nat Gas Sci Eng. https://doi.org/10.1016/j.jngse.2019.102971
8. Iloms E, Ololade OO, Ogola HJ, Selvarajan R (2020) Investigating industrial effluent impact on municipal wastewater treatment plant in Vaal, South Africa. Int J Environ Res Public Health. https://doi.org/10.3390/ijerph17031096
9. Mali SA, Zhu D, Liu Y, Gilbert JL (2021) Fretting crevice corrosion of 316 L stainless steel in physiological phosphate buffered saline: load, potential and alloy counterface effects. Tribol Int. https://doi.org/10.1016/j.triboint.2021.107198
10. Palit S (2018). In: Kharisov B (ed) Recent advances in corrosion science: a critical overview and a deep comprehension. Elsevier, Amsterdam
11. P.H.M.S.A (2020) Pipeline incident 20 year trends. In: U.S.D. Transportation (ed) Pipeline and Hazardous Materials Safety Administration, Washington, United States
12. Koch G, Varney J, Thompson N, Moghissi O, Gould M, Payer J (2016) International measures of prevention, application, and economics of corrosion technologies study, In: Jacobson G (ed) NACE International, Texas, United States, pp 1–216
13. El-Sherik AM (2017) Trends in oil and gas corrosion research and technologies: production and transmission. Woodhead Publishing, Cambridge
14. El-Haddad MA, Radwan AB, Sliem MH, Hassan WM, Abdullah AM (2019) Highly efficient eco-friendly corrosion inhibitor for mild steel in 5 M HCl at elevated temperatures: experimental & molecular dynamics study. Sci Rep. https://doi.org/10.1038/s41598-019-40149-w
15. Huang CF, Yang CY, Tsai JR, Wu CT, Liu SH, Lan KC (2018) Low-dose tributyltin exposure induces an oxidative stress-triggered JNK-related pancreatic β-cell apoptosis and a reversible hypoinsulinemic hyperglycemia in mice. Sci Rep. https://doi.org/10.1038/s41598-018-24076-w
16. Simpson N, Maaijen K, Roelofsen Y, Hage R (2019) The evolution of catalysis for alkyd coatings: responding to impending cobalt reclassification with very active iron and manganese catalysts, using polydentate nitrogen donor ligands. Catalysts. https://doi.org/10.3390/catal9100825

17. Gharbi O, Thomas S, Smith C, Birbilis N (2018) Chromate replacement: what does the future hold? NPJ Mater Degrad. https://doi.org/10.1038/s41529-018-0034-5
18. Ćwieląg-Drabek M, Piekut A, Gut K, Grabowski M (2020) Risk of cadmium, lead and zinc exposure from consumption of vegetables produced in areas with mining and smelting past. Sci Rep. https://doi.org/10.1038/s41598-020-60386-8
19. Jiang S, Wang H, Wu Y, Liu X, Chen H, Yao M, Gault B, Ponge D, Raabe D, Hirata A (2017) Ultrastrong steel via minimal lattice misfit and high-density nanoprecipitation. Nature. https://doi.org/10.1038/nature22032
20. Raabe D, Springer H, Gutiérrez-Urrutia I, Roters F, Bausch M, Seol JB, Koyama M, Choi PP, Tsuzaki K (2014) Alloy design, combinatorial synthesis, and microstructure–property relations for low-density Fe-Mn-Al-C austenitic steels. JOM. https://doi.org/10.1007/s11837-014-1032-x
21. Li D, Wang J (2018) Study of supercritical power plant integration with high temperature thermal energy storage for flexible operation. J Energy Storage. https://doi.org/10.1016/j.est.2018.09.008
22. King F (2013) Container materials for the storage and disposal of nuclear waste. Corrosion. https://doi.org/10.5006/0894
23. Zhang LC, Chen LY (2019) A review on biomedical titanium alloys: recent progress and prospect. Adv Eng Mater. https://doi.org/10.1002/adem.201801215
24. Dunn BD (2015) Materials and processes: for spacecraft and high reliability applications. Springer, Switzerland
25. Allwood JM, Cullen JM, Carruth MA, Cooper DR, McBrien M, Milford RL, Moynihan MC, Patel AC (2012) Sustainable materials: with both eyes open. UIT Cambridge Limited, Cambridge
26. Prajila M, Ammal PR, Joseph A (2018) Comparative studies on the corrosion inhibition characteristics of three different triazine based Schiff's bases, HMMT, DHMMT and MHMMT, for mild steel exposed in sulfuric acid. Egypt J Pet. https://doi.org/10.1016/j.ejpe.2017.07.011
27. Dwivedi D, Lepková K, Becker T (2017) Carbon steel corrosion: a review of key surface properties and characterization methods. RSC Adv. https://doi.org/10.1039/C6RA25094G
28. Cao Q, Esmaily M, Liu R, Birbilis N, Thomas S (2020) Corrosion of mild steel under insulation—the effect of dissolved metal ions. Corros Eng Sci Technol. https://doi.org/10.1080/1478422X.2020.1734737
29. Erna M, Herdini H, Futra D (2019) Corrosion inhibition mechanism of mild steel by amylose-acetate/carboxymethyl chitosan composites in acidic media. Int J Chem Eng. https://doi.org/10.1155/2019/8514132
30. Hou Y, Lei D, Li S, Yang W, Li C-Q (2016) Experimental investigation on corrosion effect on mechanical properties of buried metal pipes. Int J Corros. https://doi.org/10.1155/2016/5808372
31. Kim YS, Kim JG (2017) Corrosion behavior of pipeline carbon steel under different iron oxide deposits in the district heating system. Metals. https://doi.org/10.3390/met7050182
32. Jebaraj AV, Ajaykumar L, Deepak C, Aditya K (2017) Weldability, machinability and surfacing of commercial duplex stainless steel AISI2205 for marine applications—a recent review. J Adv Res. https://doi.org/10.1016/j.jare.2017.01.002
33. Tranchida G, Clesi M, Di Franco F, Di Quarto F, Santamaria M (2018) Electronic properties and corrosion resistance of passive films on austenitic and duplex stainless steels. Electrochim Acta. https://doi.org/10.1016/j.electacta.2018.04.058
34. Wang Z, Paschalidou E-M, Seyeux A, Zanna S, Maurice V, Marcus P (2019) Mechanisms of Cr and Mo enrichments in the passive oxide film on 316L austenitic stainless steel. Front Mater. https://doi.org/10.3389/fmats.2019.00232
35. Simcoe CR (2018) Stainless steel. In: Richards F (ed) The history of metals in America. ASM International, OH
36. Boillot P, Peultier J (2014) Use of stainless steels in the industry: recent and future developments. Procedia Eng. https://doi.org/10.1016/j.proeng.2014.09.015
37. Gary SW, Shigeharu U (2019) Austenitic stainless steels. In: Odette GR, Steven ZJ (ed) Structural alloys for nuclear energy applications. Newnes, Amsterdam, Netherlands
38. Klapper HS, Zadorozne NS, Rebak RB (2017) Localized corrosion characteristics of nickel alloys: a review. Acta Metall Sin. https://doi.org/10.1007/s40195-017-0553-z
39. Alwan AS, Fayyadh SK, Khalid EA (2019) A review: behavior of pitting corrosion in manufacturing food equipment. Iraqi J Agric Sci 50(4):1–7. https://doi.org/10.36103/ijas.v50i4.744
40. Niu LB, Okano K, Izumi S, Shiokawa K, Yamashita M, Sakai Y (2018) Effect of chloride and sulfate ions on crevice corrosion behavior of low-pressure steam turbine materials. Corros Sci. https://doi.org/10.1016/j.corsci.2017.12.017
41. Lindgren M, Huttunen-Saarivirta E, Peltola H, Romu J, Sarikka T, Hänninen H, Pohjanne P (2018) Crevice corrosion of stainless steels 904L, 2205, and 2507 in high-temperature sulfuric acid solution containing chlorides: influence of metal cations. Corrosion. https://doi.org/10.5006/2565
42. Gilbert JL, Zhu D (2020) A metallic biomaterial tribocorrosion model linking fretting mechanics, currents, and potentials: model development and experimental comparison. J Biomed Mater Res B: Appl Biomater. https://doi.org/10.1002/jbm.b.34643
43. Liu Y, Zhu D, Pierre D, Gilbert JL (2019) Fretting initiated crevice corrosion of 316LVM stainless steel in physiological phosphate buffered saline: potential and cycles to initiation. Acta Biomater. https://doi.org/10.1016/j.actbio.2019.07.051
44. Kuang W, Han E-H, Wu X, Rao J (2010) Microstructural characteristics of the oxide scale formed on 304 stainless steel in oxygenated high temperature water. Corros Sci. https://doi.org/10.1016/j.corsci.2010.07.015
45. Ziemniak S, Hanson M (2002) Corrosion behavior of 304 stainless steel in high temperature, hydrogenated water. Corros Sci. https://doi.org/10.1016/S0010-938X(02)00004-5
46. Lepingle V, Louis G, Allue D, Lefebvre B, Vandenberghe B (2008) Steam oxidation resistance of new 12% Cr steels: comparison with some other ferritic steels. Corros Sci. https://doi.org/10.1016/j.corsci.2007.11.033
47. Zurek J, Nieto-Hierro L, Piron-Abellan J, Niewolak L, Singheiser L, Quadakkers WJ (2004) Effect of alloying additions in ferritic 9–12% Cr steels on the temperature dependence of the steam oxidation resistance, 6th international symposium on high temperature corrosion and protection of materials. Trans Tech Publ, Embiez, France, pp 791–798
48. Nazari MH, Shi X (2018) Vehicle risks of winter road operations and best management practices. In: Shi X, Fu L (eds) Sustainable winter road operations. Wiley Online Library, Hoboken, NJ
49. Zhong ZW (2020) Advanced polishing, grinding and finishing processes for various manufacturing applications: a review. Mater Manuf Processes. https://doi.org/10.1080/10426914.2020.1772481
50. Brownlie F, Giourntas L, Hodgkiess T, Palmeira I, Odutayo O, Galloway A, Pearson A (2020) Effect of cathodic protection methods on ferrous engineering materials under corrosive wear conditions. Corros Eng Sci Technol. https://doi.org/10.1080/1478422X.2020.1742997
51. Oleiwi HM, Wang Y, Curioni M, Chen X, Yao G, Augusthus-Nelson L, Ragazzon-Smith A, Shabalin I (2018) An experimental study of cathodic protection for chloride contaminated reinforced concrete. Mater Struct. https://doi.org/10.1617/s11527-018-1273-1

52. Santos W, Brasil S, Santiago J, Telles J (2018) A new solution technique for cathodic protection systems with homogeneous region by the boundary element method. Eur J Comput Mech. https://doi.org/10.1080/17797179.2018.1439138
53. Yang M, Kainuma S, Zhuang S, Ishihara S, Kaneko A, Yamauchi T (2019) Cathodic protection system applied to steel using fiber sheet and Al-based alloy anode in atmospheric environment. Int J Electrochem Sci. https://doi.org/10.20964/2019.10.40
54. He J, Guo X, Qiao Y, Luo F (2020) A novel Zr-Y modified silicide coating on Nb-Si based alloys as protection against oxidation and hot corrosion. Corros Sci. https://doi.org/10.1016/j.corsci.2020.108948
55. Kinnunen-Raudaskoski K, Hjelt T, Kenttä E, Forsström U (2014) Thin coatings for paper by foam coating. Tappi J 13(7):9–19
56. Liu J, Cui Z, Ma D, Lu J, Cui Y, Li C, Liu W, Hao Z, Hu P, Yao M (2020) Investigation of oxidation behaviors of coated zircaloy as accident-tolerant fuel with CrAlN and CrAlSiN coatings in high-temperature steam. Corros Sci. https://doi.org/10.1016/j.corsci.2020.108896
57. Rajput A, Ak M, Kim SJ, Noh SH, Park JH, Paik JK (2019) Effects of the surface preparation on the life of epoxy coating in steel ship plates: an experimental study. Ships Offshore Struct. https://doi.org/10.1080/17445302.2019.1565072
58. Zhang F, Ju P, Pan M, Zhang D, Huang Y, Li G, Li X (2018) Self-healing mechanisms in smart protective coatings: a review. Corros Sci. https://doi.org/10.1016/j.corsci.2018.08.005
59. Zulkifli F, Yusof MSM, Isa M, Yabuki A, Nik WW (2017) Henna leaves extract as a corrosion inhibitor in acrylic resin coating. Prog Org Coat. https://doi.org/10.1016/j.porgcoat.2017.01.017
60. Parikh V, Badheka V, Badgujar A, Ghetiya N (2021) Fabrication and processing of aluminum alloy metal matrix composites. Mater Manuf Processes. https://doi.org/10.1080/10426914.2021.1914848
61. Iannuzzi M, Barnoush A, Johnsen R (2017) Materials and corrosion trends in offshore and subsea oil and gas production. npj Mater Degrad 1(1):1–1
62. Chigondo M, Chigondo F (2016) Recent natural corrosion inhibitors for mild steel: an overview. J Chem. https://doi.org/10.1155/2016/6208937
63. Faiz M, Zahari A, Awang K, Hussin H (2020) Corrosion inhibition on mild steel in 1 M HCl solution by *Cryptocarya nigra* extracts and three of its constituents (alkaloids). RSC Adv. https://doi.org/10.1039/C9RA05654H
64. Honarvar Nazari M, Shihab MS, Havens EA, Shi X (2020) Mechanism of corrosion protection in chloride solution by an apple-based green inhibitor: experimental and theoretical studies. J Infrastruct Preserv Resil. https://doi.org/10.1186/s43065-020-00007-w
65. Espinoza-Vázquez A, Rodríguez-Gómez F, Negrón-Silva G, González-Olvera R, Ángeles-Beltrán D, Palomar-Pardavé M, Miralrio A, Castro M (2020) Fluconazole and fragments as corrosion inhibitors of API 5L X52 steel immersed in 1M HCl. Corros Sci. https://doi.org/10.1016/j.corsci.2020.108853
66. Su H, Wang L, Wu Y, Zhang Y, Zhang J (2020) Insight into inhibition behavior of novel ionic liquids for magnesium alloy in NaCl solution: experimental and theoretical investigation. Corros Sci. https://doi.org/10.1016/j.corsci.2019.108410
67. Taghavikish M, Dutta NK, Roy Choudhury N (2017) Emerging corrosion inhibitors for interfacial coating. Coatings. https://doi.org/10.3390/coatings7120217
68. Goyal M, Kumar S, Bahadur I, Verma C, Ebenso EE (2018) Organic corrosion inhibitors for industrial cleaning of ferrous and non-ferrous metals in acidic solutions: a review. J Mol Liq. https://doi.org/10.1016/j.molliq.2018.02.045
69. Srivastava M, Tiwari P, Srivastava SK, Prakash R, Ji G (2017) Electrochemical investigation of Irbesartan drug molecules as an inhibitor of mild steel corrosion in 1 M HCl and 0.5 M H2SO4 solutions. J Mol Liq. https://doi.org/10.1016/j.molliq.2017.04.017
70. Tsoeunyane M, Makhatha M, Arotiba O (2019) Corrosion inhibition of mild steel by poly (butylene succinate)-L-histidine extended with 1, 6-diisocynatohexane polymer composite in 1 M HCl. Int J Corros. https://doi.org/10.1155/2019/7406409
71. Yaro AS, Khadom AA, Wael RK (2013) Apricot juice as green corrosion inhibitor of mild steel in phosphoric acid. Alex Eng J. https://doi.org/10.1016/j.aej.2012.11.001
72. Guo L, Qi C, Zheng X, Zhang R, Shen X, Kaya S (2017) Toward understanding the adsorption mechanism of large size organic corrosion inhibitors on an Fe (110) surface using the DFTB method. RSC Adv. https://doi.org/10.1039/C7RA04120A
73. Rani B, Basu BBJ (2012) Green inhibitors for corrosion protection of metals and alloys: an overview. Int J Corros. https://doi.org/10.1155/2012/380217
74. Tiu BDB, Advincula RC (2015) Polymeric corrosion inhibitors for the oil and gas industry: design principles and mechanism. React Funct Polym. https://doi.org/10.1016/j.reactfunctpolym.2015.08.006
75. Umoren SA, Solomon MM (2020) Polymeric corrosion inhibitors for oil and gas industry. In: Viswanathan SS, Saviour AU (eds) Corrosion inhibitors in the oil and gas industry. Wiley, Hoboken
76. Ali MM, Irawadi TT, Darmawan N, Khotib M, Mas'ud ZA (2019) Reaction products of crude palm oil-based fatty acids and monoethanolamine as corrosion inhibitors of carbon steel. Makara J Sci. https://doi.org/10.7454/mss.v23i3.11263
77. Elsharif AM, Abubshait SA, Abdulazeez I, Abubshait HA (2020) Synthesis of a new class of corrosion inhibitors derived from natural fatty acid: 13-docosenoic acid amide derivatives for oil and gas industry. Arab J Chem. https://doi.org/10.1016/j.arabjc.2020.03.015
78. Vázquez-Vélez E, Gonzalez-Rodriguez J, Escalante-Pérez M, Mendoza J, Martínez-Gómez L (2019) Use of fatty amide and anionic surfactant as corrosion inhibitors for carbon steel in different atmospheres. Int J Corros Scale Inhib. https://doi.org/10.17675/2305-6894-2019-8-1-11
79. Velazquez-Torres N, Martinez H, Porcayo-Calderon J, Vazquez-Velez E, Gonzalez-Rodriguez J, Martinez-Gomez L (2018) Use of an amide-type corrosion inhibitor synthesized from the coffee bagasse oil on the corrosion of Cu in NaCl. Green Chem Lett Rev. https://doi.org/10.1080/17518253.2017.1404645
80. Ahmed SK, Ali WB, Khadom AA (2019) Synthesis and investigations of heterocyclic compounds as corrosion inhibitors for mild steel in hydrochloric acid. Int J Ind Chem. https://doi.org/10.1007/s40090-019-0181-8
81. Petrunin M, Maksaeva L, Gladkikh N, Makarychev Y, Maleeva M, Yurasova T, Nazarov A (2020) Thin benzotriazole films for inhibition of carbon steel corrosion in neutral electrolytes. Coatings. https://doi.org/10.3390/coatings10040362
82. Xhanari K, Finšgar M (2019) The corrosion inhibition of AA6082 aluminium alloy by certain azoles in chloride solution: electrochemistry and surface analysis. Coatings. https://doi.org/10.3390/coatings9060380
83. Salim R, Ech-chihbi E, Oudda H, El Hajjaji F, Taleb M, Jodeh S (2019) A Review on the assessment of imidazo [1, 2-a] pyridines as corrosion inhibitor of metals. J Bio Tribo Corros. https://doi.org/10.1007/s40735-018-0207-3
84. Zhang W, Li HJ, Wang Y, Liu Y, Wu YC (2018) Adsorption and corrosion inhibition properties of pyridine-2-aldehyde-2-quinolylhydrazone for Q235 steel in acid medium:

electrochemical, thermodynamic, and surface studies. Mater Corros. https://doi.org/10.1002/maco.201810252

85. Gonzalez-Rodriguez J, Porcayo-Calderon J, Vazquez-Velez E, de la Escalera LM, Canto J, Martinez L (2016) Palm oil-based imidazolines as corrosion inhibitor for copper in 1.0 M H2SO4. J Adv Electrochem 2:97–102
86. Ismail A, Irshad H, Zeino A, Toor I (2019) Electrochemical corrosion performance of aromatic functionalized imidazole inhibitor under hydrodynamic conditions on API X65 carbon steel in 1 M HCl solution. Arab J Sci Eng. https://doi.org/10.1007/s13369-019-03745-6
87. Olajire AA (2017) Corrosion inhibition of offshore oil and gas production facilities using organic compound inhibitors—a review. J Mol Liq. https://doi.org/10.1016/j.molliq.2017.10.097
88. Wang P, Wang Y, Zhao T, Xiong C, Xu P, Zhou J, Fan Z (2020) Effectiveness protection performance of an internal blending organic corrosion inhibitor for carbon steel in chloride contaminated simulated concrete pore solution. J Adv Concr Technol. https://doi.org/10.3151/jact.18.116
89. Deyab M, Guibal E (2020) Enhancement of corrosion resistance of the cooling systems in desalination plants by green inhibitor. Sci Rep. https://doi.org/10.1038/s41598-020-61810-9
90. Fouda A, Emam A, Refat R, Nageeb M (2019) Eco-friendly plant extract of *Medicago sativa* (Alfalfa) as corrosion inhibitor for carbon steel in marine environment. Surf Eng Appl Electrochem. https://doi.org/10.3103/S1068375519030074
91. Haddadi SA, Alibakhshi E, Bahlakeh G, Ramezanzadeh B, Mahdavian M (2019) A detailed atomic level computational and electrochemical exploration of the *Juglans regia* green fruit shell extract as a sustainable and highly efficient green corrosion inhibitor for mild steel in 3.5 wt% NaCl solution. J Mol Liq. https://doi.org/10.1016/j.molliq.2019.04.045
92. Devikala S, Kamaraj P, Arthanareeswari M, Patel MB (2019) Green corrosion inhibition of mild steel by aqueous *Allium sativum* extract in 35% NaCl. Mater Today. https://doi.org/10.1016/j.matpr.2019.04.182
93. Ikhmal WMKWM, Maria MFM, Rafizah WAW, Norsani WNWM, Sabri MGM (2019) Corrosion inhibition of mild steel in seawater through green approach using *Leucaena leucocephala* leaves extract. Int J Corros Scale Inhib. https://doi.org/10.17675/2305-6894-2019-8-3-12
94. Ikhmal WMKWM, Yasmin MYN, Fazira MFM, Rafizah WAW, Nik WBW, Sabri MGM (2018) Anticorrosion coating using *Olea* sp leaves extract. IOP Conf Ser Mater Sci Eng. https://doi.org/10.1088/1757-899X/344/1/012028
95. Maria M, Ikhmal W, Amirah M, Manja S, Syaizwadi S, Chan K, Sabri M, Adnan A (2019) Green approach in anti-corrosion coating by using *Andrographis paniculata* leaves extract as additives of stainless steel 316L in seawater. Int J Corros Scale Inhib. https://doi.org/10.17675/2305-6894-2019-8-3-13
96. Loto RT, Fajobi M, Oluwole O, Loto CA (2020) Corrosion inhibition effect of calcium gluconate on mild steel in artificial seawater. Cogent Eng. https://doi.org/10.1080/23311916.2020.1712155
97. Schmitzhaus TE, Ortega Vega MR, Schroeder R, Muller IL, Mattedi S, Malfatti CdF (2020) An amino-based protic ionic liquid as a corrosion inhibitor of mild steel in aqueous chloride solutions. Mater Corros. https://doi.org/10.1002/maco.201911347
98. Moradi M, Ye S, Song Z (2019) Dual role of *Psudoalteromonas piscicida* biofilm for the corrosion and inhibition of carbon steel in artificial seawater. Corros Sci. https://doi.org/10.1016/j.corsci.2019.02.025
99. Pakiet M, Tedim J, Kowalczyk I, Brycki B (2019) Functionalized novel gemini surfactants as corrosion inhibitors for mild steel in 50 mM NaCl: experimental and theoretical insights. Colloids Surf A Physicochem Eng Asp. https://doi.org/10.1016/j.molliq.2019.04.045
100. Wang C, Chen J, Hu B, Liu Z, Wang C, Han J, Su M, Li Y, Li C (2019) Modified chitosan-oligosaccharide and sodium silicate as efficient sustainable inhibitor for carbon steel against chloride-induced corrosion. J Clean Prod. https://doi.org/10.1016/j.jclepro.2019.117823
101. Somers AE, Hinton BR, de Bruin-Dickason C, Deacon GB, Junk PC, Forsyth M (2018) New, environmentally friendly, rare earth carboxylate corrosion inhibitors for mild steel. Corros Sci. https://doi.org/10.1016/j.corsci.2018.05.017
102. Peng Y, Hughes AE, Deacon GB, Junk PC, Hinton BR, Forsyth M, Mardel JI, Somers AE (2018) A study of rare-earth 3-(4-methylbenzoyl)-propanoate compounds as corrosion inhibitors for AS1020 mild steel in NaCl solutions. Corros Sci. https://doi.org/10.1016/j.corsci.2018.09.022
103. Talebian M, Raeissi K, Atapour M, Fernández-Pérez B, Salarvand Z, Meghdadi S, Amirnasr M, Souto R (2018) Inhibitive effect of sodium (E)-4-(4-nitrobenzylideneamino) benzoate on the corrosion of some metals in sodium chloride solution. Appl Surf Sci. https://doi.org/10.1016/j.apsusc.2018.04.073
104. Dehghani A, Bahlakeh G, Ramezanzadeh B (2019) A detailed electrochemical/theoretical exploration of the aqueous Chinese gooseberry fruit shell extract as a green and cheap corrosion inhibitor for mild steel in acidic solution. J Mol Liq. https://doi.org/10.1016/j.molliq.2019.03.011
105. Fernandes CM, Fagundes TdSF, dos Santos NE, Rocha TSdM, Garrett R, Borges RM, Muricy G, Valverde AL, Ponzio EA (2019) *Ircinia strobilina* crude extract as corrosion inhibitor for mild steel in acid medium. Electrochim Acta. https://doi.org/10.1016/j.electacta.2019.04.148
106. Divya P, Subhashini S, Prithiba A, Rajalakshmi R (2019) *Tithonia diversifolia* flower extract as green corrosion inhibitor for mild steel in acid medium. Mater Today. https://doi.org/10.1016/j.matpr.2019.05.252
107. Salhi A, Hamdani I, Bouyanzer A, Chahboun N, Amhamdi H, Warad I, Hammouti B, Bentiss F, Zarrouk A (2018) Phytochemical analysis, antioxidant and anticorrosive activities of *Thymus algeriensis* extracts. Anal Bioanal Electrochem 10:1587–1610
108. Ramezanzadeh M, Bahlakeh G, Sanaei Z, Ramezanzadeh B (2018) Studying the Urtica dioica leaves extract inhibition effect on the mild steel corrosion in 1 M HCl solution: complementary experimental, ab initio quantum mechanics, Monte Carlo and molecular dynamics studies. J Mol Liq. https://doi.org/10.1016/j.molliq.2018.09.059
109. Liao LL, Mo S, Luo HQ, Li NB (2018) Corrosion protection for mild steel by extract from the waste of lychee fruit in HCl solution: experimental and theoretical studies. J Colloid Interface Sci. https://doi.org/10.1016/j.jcis.2018.02.071
110. Alibakhshi E, Ramezanzadeh M, Bahlakeh G, Ramezanzadeh B, Mahdavian M, Motamedi M (2018) *Glycyrrhiza glabra* leaves extract as a green corrosion inhibitor for mild steel in 1 M hydrochloric acid solution: experimental, molecular dynamics, Monte Carlo and quantum mechanics study. J Mol Liq. https://doi.org/10.1016/j.molliq.2018.01.144
111. Cordeiro RF, Belati AJ, Perrone D, D'Elia E (2018) Coffee husk as corrosion inhibitor for mild steel in HCl media. Int J Electrochem Sci. https://doi.org/10.20964/2018.12.29
112. Singh P, Chauhan D, Chauhan S, Singh G, Quraishi M (2019) Chemically modified expired Dapsone drug as environmentally benign corrosion inhibitor for mild steel in sulphuric acid useful for industrial pickling process. J Mol Liq. https://doi.org/10.1016/j.molliq.2019.110903
113. Verma C, Obot I, Bahadur I, Sherif E-SM, Ebenso EE (2018) Choline based ionic liquids as sustainable corrosion inhibitors on mild steel surface in acidic medium: gravimetric,

electrochemical, surface morphology, DFT and Monte Carlo simulation studies. Appl Surf Sci. https://doi.org/10.1016/j.apsusc.2018.06.035

114. Rabizadeh T, Khameneh-Asl S (2019) Chitosan as a green inhibitor for mild steel corrosion: thermodynamic and electrochemical evaluations. Mater Corros. https://doi.org/10.1002/maco.201810501
115. Ahmed MHO, Al-Amiery AA, Al-Majedy YK, Kadhum AAH, Mohamad AB, Gaaz TS (2018) Synthesis and characterization of a novel organic corrosion inhibitor for mild steel in 1 M hydrochloric acid. Results Phys. https://doi.org/10.1016/j.rinp.2017.12.039
116. Al-Fakih AM, Abdallah HH, Aziz M (2019) Experimental and theoretical studies of the inhibition performance of two furan derivatives on mild steel corrosion in acidic medium. Mater Corros. https://doi.org/10.1002/maco.201810221
117. Idouhli R, Koumya Y, Khadiri M, Aityoub A, Abouelfida A, Benyaich A (2019) Inhibitory effect of *Senecio anteuphorbium* as green corrosion inhibitor for S300 steel. Int J Ind Chem. https://doi.org/10.1007/s40090-019-0179-2
118. Liu L, Cao TT, Zhang QW, Cui CW (2018) Organic phosphorus compounds as inhibitors of corrosion of carbon steel in circulating cooling water: weight loss method and thermodynamic and quantum chemical studies. Adv Mater Sci Eng. https://doi.org/10.1155/2018/1653484
119. Xavier Stango SA, Vijayalakshmi U (2018) Studies on corrosion inhibitory effect and adsorption behavior of waste materials on mild steel in acidic medium. J Asian Ceram Soc. https://doi.org/10.1080/21870764.2018.1439608
120. Faisal M, Saeed A, Shahzad D, Abbas N, Larik FA, Channar PA, Fattah TA, Khan DM, Shehzadi SA (2018) General properties and comparison of the corrosion inhibition efficiencies of the triazole derivatives for mild steel. Corros Rev. https://doi.org/10.1515/corrrev-2018-0006
121. Varvara S, Găină L, Bostan R, Popa F, Grozav A (2018) Some phenothiazinyl-thiazolyl-hydrazine derivatives as corrosion inhibitors for carbon steel in 1.0 m HCl: electrochemical, SEM-EDX and DFT investigations. Int J Electrochem Sci. https://doi.org/10.20964/2018.09.32
122. Deng S, Li X, Xie X (2014) Hydroxymethyl urea and 1, 3-bis (hydroxymethyl) urea as corrosion inhibitors for steel in HCl solution. Corros Sci. https://doi.org/10.1016/j.corsci.2013.11.041
123. Verma C, Quraishi M, Olasunkanmi L, Ebenso EE (2015) L-Proline-promoted synthesis of 2-amino-4-arylquinoline-3-carbonitriles as sustainable corrosion inhibitors for mild steel in 1 M HCl: experimental and computational studies. RSC Adv. https://doi.org/10.1039/C5RA16982H
124. Verma C, Quraishi M, Singh A (2016) A thermodynamical, electrochemical, theoretical and surface investigation of diheteroaryl thioethers as effective corrosion inhibitors for mild steel in 1 M HCl. J Taiwan Inst Chem Eng. https://doi.org/10.1016/j.jtice.2015.06.020
125. Verma CB, Quraishi M, Singh A (2015) 2-Aminobenzene-1,3-dicarbonitriles as green corrosion inhibitor for mild steel in 1 M HCl: electrochemical, thermodynamic, surface and quantum chemical investigation. J Taiwan Inst Chem Eng. https://doi.org/10.1016/j.jtice.2014.11.029
126. Frolenkova S, Overchenko T, Motronyuk T, Vorobyova V, Miroshnychenko I, Panchenko M (2019) Passivating anions effect on the anodic behavior of steel in a converting acetate solution. J Chem Technol Metall 54(2):443–446
127. Tang Z (2019) A review of corrosion inhibitors for rust preventative fluids. Curr Opin Solid State Mater Sci. https://doi.org/10.1016/j.cossms.2019.06.003
128. Yang Z, Guo M, Wang N, Ma C, Wang J, Han M (2017) A short review of cathode poisoning and corrosion in solid oxide fuel cell. Int J Hydrog Energy. https://doi.org/10.1016/j.ijhydene.2017.08.057
129. Kundu SS, Seiersten M (2017) Development of a non-sulphite oxygen scavenger for monoethylene glycol (MEG) used as gas hydrate inhibitor. J Pet Sci Eng. https://doi.org/10.1016/j.petrol.2017.07.041

Authors and Affiliations

Wan Mohamad Ikhmal Wan Mohamad Kamaruzzaman[1,2] · Nursabrina Amirah Mohd Nasir[1,2] · Nur Aiman Syafiq Mohd Hamidi[1,2] · Nusaibah Yusof[1,2] · Muhamad Syaizwadi Shaifudin[1,2] · Abdul Muiz Aniq Aiman Mohd Suhaimi[1,2] · Malia Athirah Badruddin[1,2] · Wan Mohd Norsani Wan Nik[2,3] · Mohammad Fakhratul Ridwan Zulkifli[2,3] · Azila Adnan[1] · Wan Rafizah Wan Abdullah[2,3] · Mohd Hafiz Mohd Zaid[4] · Khamirul Amin Matori[4] · Chen Soo Kien[4] · Pierluigi Traverso[5] · Roberto Stifanese[5] · Jiyaul Haque[6] · Mohd Sabri Mohd Ghazali[1,2]

Wan Mohamad Ikhmal Wan Mohamad Kamaruzzaman
ikhmal007@gmail.com

Nursabrina Amirah Mohd Nasir
sabrinaamirah38@gmail.com

Nur Aiman Syafiq Mohd Hamidi
aimansyafiq140@gmail.com

Nusaibah Yusof
nusaibah@umt.edu.my

Muhamad Syaizwadi Shaifudin
syaizwadi@gmail.com

Abdul Muiz Aniq Aiman Mohd Suhaimi
abdulmuiz97@gmail.com

Malia Athirah Badruddin
maliaathirah98@gmail.com

Wan Mohd Norsani Wan Nik
niksani@umt.edu.my

Mohammad Fakhratul Ridwan Zulkifli
fakhratul@umt.edu.my

Azila Adnan
azila.adnan@umt.edu.my

Wan Rafizah Wan Abdullah
wanrafizah@umt.edu.my

Mohd Hafiz Mohd Zaid
mhmzaid@upm.edu.my

Khamirul Amin Matori
khamirul@upm.edu.my

Chen Soo Kien
chensk@upm.edu.my

Pierluigi Traverso
pierluigi.traverso@ias.cnr.it

Roberto Stifanese
roberto.stifanese@ias.cnr.it

Jiyaul Haque
jiyaulh.rs.chy15@itbhu.ac.in

[1] Faculty of Science and Marine Environment, Universiti Malaysia Terengganu, 21030 Kuala Nerus, Terengganu, Malaysia

[2] Materials and Corrosion Research Group, Universiti Malaysia Terengganu, 21030 Kuala Nerus, Terengganu, Malaysia

[3] Faculty of Ocean Engineering Technology and Informatics, Universiti Malaysia Terengganu, 21030 Kuala Nerus, Terengganu, Malaysia

[4] Department of Physics, Faculty of Science, Universiti Putra Malaysia, Seri Kembangan, UPM Serdang, 43400 Serdang, Malaysia

[5] Genoa Department, Institute of Anthropic Impacts and Sustainability in Marine Environment (CNR-IAS), Via De Marini, 6 -IV Floor, 16149 Genoa, Italy

[6] Department of Chemistry, IIT(BHU), Varanasi 221005, India